NACA

# RESEARCH MEMORANDUM

## FLAME VELOCITIES OVER A WIDE COMPOSITION RANGE FOR PENTANE-AIR, ETHYLENE-AIR, AND PROPYNE-AIR FLAMES

By Dorothy M. Simon and Edgar L. Wong

Lewis Flight Propulsion Laboratory
Cleveland, Ohio



NATIONAL ADVISORY COMMITTEE
FOR AERONAUTICS

WASHINGTON
October 18, 1951

NATIONAL ADVISORY COMMITTEE FOR AERONAUTICS

RESEARCH MEMORANDUM

# FLAME VELOCITIES OVER A WIDE COMPOSITION RANGE FOR PENTANE-AIR, ETHYLENE-AIR, AND PROPYNE-AIR FLAMES

By Dorothy M. Simon and Edgar L. Wong



## SUMMARY

The change in flame velocity with fuel concentration in air was investigated in order to determine whether an active particle diffusion mechanism of flame propagation is consistent with the observed velocity changes, and to show whether the simplified diffusion mechanism as expressed by the Tanford and Pease equation is sufficiently exact to predict the velocity change with fuel concentration in air. Spatial flame velocities were measured for nearly the total flammability range for pentane-air, ethylene-air, and propyne-air mixtures by a modified tube method at atmospheric pressure and 25° C. Flame shape as revealed by direct photographs was studied. Flame front areas were measured from the direct photographs for different fuel concentrations in air. Fundamental flame velocities were calculated for the concentration range from 60 to 130 percent stoichiometric for the three hydrocarbons. Equilibrium flame temperatures and equilibrium free radical concentrations were calculated for pentane, ethylene, and propyne over the total flammability range in air. The velocity measurements together with these calculated concentrations were used for a quantitative evaluation of the active particle diffusion theory. It is shown that a general diffusion mechanism is consistent with the observed changes in flame velocity with fuel concentration, and that a form of the Tanford and Pease equation which includes a flame velocity term independent of diffusion will predict the velocity changes over a limited concentration range.

## INTRODUCTION

One of the important processes in a jet-engine combustor is the propagation of flame into the unburned fuel-air mixture. A better understanding of the physical and chemical nature of this process may be gained by a study of laminar flame speeds.

A research program is in progress at the NACA Lewis laboratory to determine the effect of chemical structure on the maximum flame velocity of fuel-air mixtures. The maximum flame velocities of all 52 hydrocarbons studied are reported (references 1 and 2) to be consistent with

an active particle mechanism of flame propagation. It is also shown in references 1 and 2 that the simplified active particle mechanism of flame propagation as expressed by a modified equation of the type proposed by Tanford and Pease (reference 3) could be used, with one specific rate constant, to predict the maximum flame velocities for all of the hydrocarbons except ethylene. In order to determine whether the change in flame velocity with fuel concentration in air is also consistent with an active particle diffusion mechanism of flame propagation and whether the modified Tanford and Pease expression is sufficiently accurate to predict this change, flame velocities must be known over a wide concentration range.



Fundamental flame velocities are presented herein for three hydrocarbons of different chemical structure, pentane, ethylene, and propyne, over a wide composition range in air. These three hydrocarbons were chosen for different reasons. Propyne was chosen so that the total flame velocity range previously studied (references 1 and 2) for different hydrocarbon-air mixtures would be produced by one hydrocarbon in varying concentrations in air. Ethylene was used because the previous work indicated that the behavior of ethylene differed from other hydrocarbons. Pentane was studied as a representative of the paraffin family and a compound of low maximum flame velocity.

Equilibrium flame temperatures and equilibrium product concentrations of hydrogen atoms, oxygen atoms, and hydroxyl radicals are also reported. The results of these calculations together with the experimental flame velocities are used to evaluate quantitatively the active particle diffusion theory of flame propagation. None of the other proposed theories of propagation as developed by Semenov, Zeldovich, and Frank-Kemenetsky, (references 4, 5, and 6), Hirschfelder (reference 7), Bechert (reference 8), or Manson (reference 9), are considered in this report.

## APPARATUS AND PROCEDURE

Spatial flame velocities were measured at atmospheric pressure and room temperature (25° to 30° C) by the modified tube method reported by Gerstein, Levine, and Wong (reference 10). The apparatus consisted of a fuel measuring and mixing system, a fuel transfer system, and a horizontal cylindrical flame tube. The pyrex flame tube was 2.5 centimeters in inside diameter and 60 centimeters long with an orifice at each end. The diameter of the orifice at the ignition end of the tube was 8 millimeters and at the other end was 1.7 millimeters. An alcohol lamp was used for ignition.

For each combustible mixture the time required for the flame to travel between two fixed points in the flame tube was determined, and direct photographs of the moving flame front were taken. The time for the flame to travel 17.8 centimeters in the tube was measured by a photoelectric timer consisting of two photoelectric flame detectors, two pulse shapers, a signal generator, a timer gate, and an electronic counter as shown in the block diagram (fig. 1(a)). In practice, the last three components are integral parts of a Potter interval timer, model 451B. This timing device is sensitive enough to detect the pale flames which occur near the lean concentration limit of propagation. A diagram of the circuit for the flame detectors is presented in figure 1(b). The pulse shaping circuit is shown in figure 1(c). The electronic timing equipment, which was designed and built by Edward R. Carlson of the Lewis laboratory, is described in appendix A. Direct photographs were made of flames at each fuel concentration with a motion-picture camera which was maintained in a fixed position for all mixtures. The flame fronts were recorded on 16-millimeter film with a camera speed of 64 frames per second.



The source and the purity of the three hydrocarbons are given in table I. The air used for the combustible mixtures was laboratory air dried by passage through two 8-inch drying towers containing Anyhydrone and freed of carbon dioxide by passage through an Ascarite tower.

## RESULTS AND DISCUSSION

### Spatial Flame Velocities

Spatial flame velocities were measured for three hydrocarbons, pentane, ethylene, and propyne, over nearly the total flammability range for each hydrocarbon in air. The measured spatial flame velocities are plotted against fuel concentration expressed as percent stoichiometric in figure 2. The curves for ethylene and propyne are very similar, whereas pentane has a lower maximum flame velocity and a narrower flammability region.

The arrows represent the concentration limits for propagation as determined in this work. These limits are narrower than the limits reported by Coward and Jones (reference 11) of 53 and 321 percent of stoichiometric for pentane and 44 and 581 percent of stoichiometric for ethylene. The difference in the limits is in the direction which would be predicted from the difference in the method of determining the limits (reference 11). The limits reported by Coward and Jones are for upward propagation in a tube 5.0 centimeters in diameter, whereas the limits presented in this report are for horizontal propagation in a tube 2.5 centimeters in diameter.

Fundamental flame velocities may be calculated from the spatial flame velocities by the equation of Coward and Payman (reference 12)

$$U_f = (U_o - U_g)\, A_t/A_f \qquad (1)$$

where

$U_f$ fundamental flame velocity, which is defined as velocity component normal to any tangent to flame surface, (cm/sec)

$U_o$ spatial flame velocity, (cm/sec)

$U_g$ gas velocity, (cm/sec)

$A_t$ cross-sectional area of flame tube, (sq cm)

$A_f$ flame front area, (sq cm)

(All symbols are also defined in appendix B.)

Spatial velocities are the measured velocities just discussed. The gas velocity was calculated from the empirical equation reported in reference 10.

$$U_g = 0.236\, U_o - 10.47 \qquad (2)$$

The flame tube cross-sectional area was calculated from the measured diameter of the tube, and the flame front area was determined from the direct photographs of the flames.



## Measurement of Flame Front Area

The measurement of flame front areas presents a difficult problem. The flame shape as recorded photographically changed with fuel composition. Typical flame photographs showing this change with concentration are given in figure 3. These photographs are for propyne-air mixtures; however, similar changes in flame shape were observed for pentane-air and ethylene-air mixtures. The flame front appeared to lengthen, particularly near the bottom of the flame tube, as fuel concentration increased from the lean limit to 180 percent of stoichiometric. For a very short concentration range above 180 percent, the flame shape returned to a form similar to the very lean flame shapes, and then the flame abruptly changed to a very long front which did not fill the flame

tube. The last photograph of the regular flame shape series (fig. 3(a)) shows one of these long flames with the bottom of the flame tube defined by light reflected from the flame. Not only were these regular flame shapes observed, but occasionally very different flames appeared. Three examples of these irregular flames are shown in figure 3(b). Such flame shapes were frequently observed near the maximum flame velocity for propyne and ethylene, but they were seldom observed for pentane at any concentration. Only regular flame shapes were used for area calculations.



In order to calculate areas from the photographs, an arbitrary geometric figure was chosen to represent the flame. As in reference 13 by Coward and Hartwell an ellipsoid of revolution was used. Three axes of the ellipsoid were measured and the area was calculated by the general formula for an ellipsoid of revolution determined by three axes. The method of choosing the axes is shown in figure 4, which represents an outline trace of a flame photograph with the axes of the ellipsoid, which were used for the area calculation, constructed on it. One axis is the line AB, which connects the two points of tangency of the flame and the flame tube, the second axis is twice the line CD, which is the longest perpendicular from the line AB to the flame front, and the third is the diameter of the flame tube BE. The flame front was considered to be a semiellipsoid.

In order to measure the flame areas, the projected negative of a flame front was superimposed on the image of a flame tube which had been traced. The two were properly oriented by lining up the sprocket holes in the negative with those which had been traced for the flame tube negative. The flame front was traced ten times, the axes of the ellipsoid constructed and measured, and the average area calculated. Unfortunately the calculated area is very sensitive to the choice of the points of tangency of the flame to the tube. One person can use the method of area measurement for flame fronts from mixtures of constant composition with a reproducibility of ±3 percent, but if a second person measures the same flame fronts the two average area values may differ by as much as 15 percent. The areas evaluated by one individual are believed to be relatively correct, but the absolute value of the area is not established.

The calculated average relative areas are plotted against hydrocarbon concentration in air for pentane, ethylene, and propyne mixtures in figure 5. Each point is the average of several calculated areas. Areas for mixtures much richer than 140 percent of stoichiometric were so uncertain that they could not be used. It may be observed that the type of hydrocarbon in the combustible mixtures does not change the flame front area within the limits of the measurements. Although the change in area with the concentration of hydrocarbon in air is not large and there is considerable scatter in the data, a curve has been drawn.

The change in flame front area with composition as shown by this curve is similar to the change in area with composition reported by Burke and Friedman (reference 14) for acetylene and dideuteroacetylene-air mixtures. If the best horizontal straight line were drawn in figure 5 instead of the curve, the adjusted fundamental velocities calculated from the line would not be significantly different from the adjusted velocities presented later in this report.

## Relative Fundamental Flame Velocities



Relative fundamental flame velocities for ethylene were calculated by the Coward and Payman equation using areas read from the curve in figure 5. These values are plotted against fuel concentration in air expressed as percent of stoichiometric in figure 6(a). Bunsen burner flame velocities for ethylene-air mixtures determined by Linnett and Hoare (reference 15) and revised (reference 16) are also plotted on the same graph. The fundamental flame velocities for ethylene calculated from the measured flame areas are relatively correct, but these velocities reflect the 15-percent uncertainty in the absolute area.

## Adjusted Fundamental Flame Velocities

In order to compare the relative fundamental flame velocities determined by the tube method with fundamental flame velocities determined by other methods, the tube velocities may be adjusted by a constant factor to compensate for the uncertainty in the measurement of the absolute area of the flame front. The adjustment was accomplished by using the maximum value for the flame velocities of ethylene determined by the Bunsen burner method from the shadow cone (reference 16) as a standard. The relative fundamental flame velocities calculated in this report were adjusted by multiplying the relative values by the ratio of the maximum fundamental flame velocity for ethylene by the Bunsen burner method to the maximum flame velocity for ethylene calculated in this report, or by 1.076. These adjusted fundamental flame velocities for ethylene and the data for ethylene of Linnett and Hoare are plotted in figure 6(b). The change in fundamental flame velocity with ethylene concentration in air as measured by the tube method is shown to compare favorably with the Bunsen burner values.

Relative fundamental flame velocities for propyne and pentane were calculated by equation (1) and adjusted by multiplying the relative value by 1.076. The adjusted fundamental flame velocities for pentane, ethylene, and propyne are plotted against hydrocarbon composition in air expressed as percent of stoichiometric in figure 7. In table II, all spatial flame velocities, relative fundamental velocities, and adjusted fundamental flame velocities are tabulated. The adjusted fundamental flame velocities are consistent with the fundamental flame velocities which are reported in references 10, 17, and 18.

## THEORY

### General Discussion

A general theory of flame propagation would include all the processes which may occur in a flame like diffusion of free radicals, conduction of heat, and chemical oxidation. Hirschfelder and Curtis (reference 7) have formulated such a general theory of flame propagation. It would be desirable to use this general theory to compare the calculated effect of the composition of the combustible mixtures on the fundamental flame velocity with the experimentally observed effects for hydrocarbon-air mixtures. But in order to make any calculations, the chemical kinetic system and reaction rates for oxidation must be known. Because the chemical kinetics of hydrocarbon oxidation are not established, it might be hoped to use the general theory and the observed effects of changing initial conditions on the fundamental flame velocity to work backward to the kinetics of the oxidation reaction. Unfortunately, the mathematics are so involved and the chemical reactions so complicated that the general approach does not appear to be very promising.

There are, however, two types of simplified theory of flame propagation: theories based primarily on heat conduction like those of Semenov, Zeldovich, and Frank-Kemenetsky (references 4, 5, and 6) and Bechert (reference 8); and theories based on diffusion of active particles like those of Lewis and von Elbe (reference 19) and Tanford and Pease (reference 3). The second type of simplified theory only is considered in this report because an equation of this type may be numerically evaluated and a simplified equation has been successfully used to predict the maximum flame velocities for hydrocarbon-air flames (references 1 and 2).

### Active Particle Diffusion Mechanism

According to the diffusion mechanism, flame propagates by the diffusion of light chemically active particles such as hydrogen atoms, oxygen atoms, and hydroxyl radicals. These active particles are the carriers of the chain reactions which give rise to the visible flame. Several difficulties are encountered in attempting to relate the rate of flame propagation, the process of diffusion, and the chemical-reaction mechanism of oxidation. By making some simplifying assumptions, Tanford and Pease (references 3 and 20) have derived an expression relating fundamental flame velocity and the active particle concentration ahead of the flame. The equation is

$$U_f = \left( \frac{Q' L}{Q} \Sigma_i \, k_i \, \frac{D_i \, P_i}{B_i} \right)^{1/2} \qquad (3)$$

where

$U_f$ fundamental flame velocity, (cm/sec)

Q' mole fraction of combustible

L number of molecules of gas at reaction temperature, (molecules/cc)

Q mole fraction of potential combustion product

$k_i$ specific rate constant for reaction of combustible and the $i^{th}$ active particle, (cc molecules$^{-1}$ sec$^{-1}$)

$D_i$ rate of diffusion of the $i^{th}$ active particle, (cm$^2$ sec$^{-1}$)

$P_i$ partial pressure of the $i^{th}$ active particle, (atm)

$B_i$ term arising from recombination of the $i^{th}$ active particles

This expression was used successfully by Tanford (reference 21) to predict the flame velocities of $CO-O_2-N_2-H_2O$, $CH_4-O_2-N_2$, and $H_2-O_2-N_2$ mixtures. A modified equation of the same type with one specific rate constant was shown in reference 1 to predict the maximum flame velocities of the 52 hydrocarbon-air mixtures which were studied.

## Atom and Free Radical Concentrations and Equilibrium Flame Temperatures

In order to compare the experimentally observed effect of changes in fuel concentration in air on the fundamental flame velocity with the effect predicted by a Tanford and Pease type equation, the concentration of active particles in the flame must be known. This concentration is assumed to be the equilibrium concentration calculated for the equilibrium flame temperature. Although this assumption may be an over simplification, there is insufficient knowledge of the oxidation reaction to calculate the concentrations by any other method. Equilibrium, active particle concentrations and adiabatic, equilibrium flame temperatures were calculated simultaneously by the matrix method of Huff and Morrell (reference 22). The tables of thermodynamic constants published by Huff and Gordon (reference 23) and the heats of formation published by the Bureau of Standards (reference 24) were used for these calculations. The first estimates for the matrix calculations for flame temperature were made by the method of Hottel, Williams, and Satterfield (reference 25) and the first estimates for equilibrium product concentrations were calculated by the method of Huff and Calvert (reference 26). The results of these calculations together with a consideration of the diffusion coefficients indicate that hydrogen atoms

are probably the most important oxidation chain carriers but that oxygen atoms and hydroxyl radicals could also be important. These three particles only are considered in the diffusion mechanism of flame propagation. The calculated equilibrium flame temperatures and the equilibrium concentrations of hydrogen atoms, oxygen atoms, and hydroxyl radicals for pentane, ethylene, and propyne mixtures with air are given in table III.



The calculated equilibrium flame temperatures are plotted against hydrocarbon concentration in air expressed as percent of stoichiometric in figure 8. The maximum flame temperatures occur at concentrations somewhat richer than stoichiometric. The concentrations for maximum flame velocity are shown by the arrows on the curves in figure 8. The fuel concentrations for the maximum flame velocities are near the concentrations for the maximum calculated flame temperatures. These data are consistent with the report that the observed maximum flame temperature for ethylene occurs near 103-percent stoichiometric, whereas the maximum flame velocity is obtained for a mixture slightly richer in ethylene (reference 27).

The calculated active particle concentrations are plotted against hydrocarbon concentration in air expressed as percent of stoichiometric for pentane for the concentration range 50 to 125 percent in figure 9(a), for ethylene for 45 to 250 percent in figure 9(b), and for propyne for 45 to 210 percent in figure 9(c). The decreasing order of maximum concentration for the active particles is hydroxyl radicals, hydrogen atoms, and oxygen atoms for the three hydrocarbons. The maximum oxygen and hydroxyl concentrations occur near the stoichiometric concentration, whereas the maximum hydrogen-atom concentration occurs on the rich side of the stoichiometric concentration between 120 and 140 percent. The concentration of fuel in air for the maximum flame velocity is designated by the arrow and is between 110 and 120 percent of stoichiometric for these three hydrocarbons.

A comparison of the hydrogen-atom concentrations for the three hydrocarbon fuels is presented in figure 9(d). Because hydrogen atoms are light, they diffuse faster than the other free radicals and are therefore most important to a diffusion mechanism of flame propagation. Although propyne and ethylene in air have approximately the same flame velocity over a wide composition range, the hydrogen-atom concentrations are quite different. This fact is consistent with the observation that the behavior of ethylene appears to differ from other hydrocarbons (references 1 and 2). In the study of the maximum flame velocities of hydrocarbons, it was shown that active particles are more effective in promoting the propagation of the ethylene-air flames than any other hydrocarbon-air flames which have been studied. It may also be noted that the equilibrium concentration of hydrogen atoms has reached a very low value considerably before the lean concentration limit is reached; this fact suggests that hydroxyl radicals and oxygen atoms must play a more important role near the lean limit of flame propagation if diffusion determines this limit.

## Evaluation of a General Diffusion Mechanism

If the diffusion of active particles is important in the propagation of flames, the relative diffusion concentration of active particles, which may be expressed as the product of the relative diffusion coefficients in air multiplied by the concentration of active particles ($6.5\ P_H + P_O + P_{OH}$), should correlate with the flame velocity. The fundamental flame velocities are plotted against the relative diffusion concentration of active particles in figure 10. One curve is defined for each hydrocarbon. Linnett and Hoare (references 15 and 16) showed a similar correlation for ethylene-air-nitrogen and ethylene - air - carbon-dioxide mixtures.



The correlation between maximum flame velocity and relative diffusion concentration of active particles for 52 hydrocarbons at the concentration of the maximum flame velocity (references 1 and 2) is shown by the line in figure 11. Although the line was originally drawn for paraffin, cycloparaffin, olefin, diolefin, and acetylene hydrocarbons, only three data points are shown - pentane, ethylene, and propyne. A comparison of figures 10 and 11 shows that the curve of flame velocity against relative active particle concentration for propyne mixtures does not follow the curve for the various hydrocarbons as might have been expected.

## Evaluation of Tanford and Pease Equation

A general diffusion mechanism appeared to correlate the velocity data; therefore the simplified theory expressed by the Tanford and Pease equation was quantitatively evaluated. In deriving the Tanford and Pease equation, which relates the flame velocity and the diffusion concentration of active particles, it was assumed that the oxidation chain reaction is initiated by the reaction of an active particle and a fuel molecule. In order to apply this equation to the hydrocarbon data, it was also assumed that the specific rate of the initiation reaction is the same whether hydrogen atoms, oxygen atoms, or hydroxyl radicals are the initiating species. The modified equation, which was applied to hydrocarbon-air mixtures (references 1 and 2), is

$$U_f = \left[ \frac{n\ Q'L}{Q}\ k \left( \frac{D_H\ P_H}{B_H} + D_O\ P_O + D_{OH}\ P_{OH} \right) \right]^{1/2} \qquad (4)$$

where

$n$ number of molecules of final combustion products (combined $CO_2$ and $H_2O$) per molecule of fuel

$k$ average specific rate constant for reaction of active particles and hydrocarbon molecules, (cc molecules$^{-1}$ sec$^{-1}$)

$D_H$ diffusion coefficient for hydrogen atoms into air at room temperature, (cm$^2$ sec$^{-1}$)

$P_H$ partial pressure of hydrogen atoms, (atm)

$B_H$ recombination factor for hydrogen atoms, (atm)

$D_O$ diffusion coefficient for oxygen atoms into air at room temperature, (cm$^2$ sec$^{-1}$)

$P_O$ partial pressure of oxygen atoms, (atm)

$D_{OH}$ diffusion coefficient for hydroxyl radicals into air at room temperature, (cm$^2$ sec$^{-1}$)

$P_{OH}$ partial pressure of hydroxyl radicals, (atm)

The term $B_H$ was evaluated according to the method of Tanford (reference 20) by considering the reactions

$$H + H + M \rightarrow H_2 + M$$

$$H + O_2 \rightarrow HO_2$$

The equation used was

$$B_H = \frac{1}{2}\left\{1 + \left[1 + \frac{24{,}000\ D_H}{U_f\ \theta_m^{\,2}}\left(q_{O_2} + 1850\ P_H\right)\right]^{1/2}\right\}$$

where

$\theta_m$ 0.7 of equilibrium temperature over initial temperature

$q_{O_2}$ 0.5 of the factor initial mole fraction of $O_2$ minus the final mole fraction of $O_2$

The diffusion coefficients of the active particles into air at the initial temperature of 25° C were calculated by kinetic theory using the Stefan-Maxwell equation (reference 28).

$$D = \frac{2}{3\pi (N_1 + N_2) \sigma^2} \sqrt{\frac{1}{h\pi}\left(\frac{1}{m_1} + \frac{1}{m_2}\right)} \qquad (5)$$

where

D diffusion coefficient

$N_1, N_2$ molecular densities

$\sigma$ arithmetic average of molecular diameters of diffusing gases

h $1/2kT$

$m_1, m_2$ molecular masses

One-half of the diffusion diameter for oxygen molecules into air was used as the diffusion diameter for oxygen atoms, the Bohr radius was used for the hydrogen-atom diffusion diameter, and the sum of the two was used for hydroxyl radicals. The diffusion coefficients were calculated to be 1.8 square centimeters per second for hydrogen atoms into air, 0.28 square centimeter per second for hydroxyl radicals, and 0.40 square centimeter per second for oxygen atoms into air at 25° C.

As a first approximation $\frac{n\ Q'L\ k}{Q}$ may be assumed constant for the total concentration range. The Tanford and Pease equation predicts that the flame velocity plotted against the square root of the relative diffusion concentration of active particles should be a straight line. These data are presented for ethylene, propyne, and pentane in figure 12. The best straight lines have been drawn by the least-squares method. These lines do not go through the origin; therefore to predict the change in flame velocity with fuel concentration in air, the intercept must be included. The equation for flame velocity must be modified to the following form:

$$U_f = U_0 + \left[\frac{n\ Q'L}{Q}\ k\left(\frac{P_H\ D_H}{B_H} + P_O\ D_O + P_{OH}\ D_{OH}\right)\right]^{1/2} \qquad (6)$$

where

$U_0$ intercept of curve and is 5.8 centimeters per second for pentane, 15.1 for ethylene, and 16.5 for propyne

The value of k was calculated for each experimental velocity without a temperature correction. These values were averaged and the average was used to calculate flame velocities for each hydrocarbon system. The experimental flame velocities are compared with the calculated velocities in table IV. The fact that the flame velocities may be so well predicted by the equation does not necessarily mean that the simplified diffusion mechanism is operative. The physical significance of the necessity for including a constant term $U_0$, a flame velocity which is independent of a diffusion mechanism, is difficult to ascertain. Certainly the $U_0$ term appears to mean that the hydrocarbon-air mixtures can support combustion in the absence of active particles; this term could be a correction for a second process which is important to flame propagation and is more important at low flame speeds near the limit of flame propagation. On the other hand, the necessity for including a constant term may have no physical significance but may only indicate that the diffusion mechanism, as expressed by the Tanford and Pease equation, with an average specific rate constant, is not exact enough to explain the change in flame velocity with fuel concentration in air for these hydrocarbons.



## CONCLUDING REMARKS

The investigation of flame velocities over a wide concentration range for pentane-air, ethylene-air, and propyne-air flames may be summarized as follows:

1. The modified tube method for the measurement of laminar flame velocities was extended for use with slow flames of low luminosity.

2. Spatial flame velocities were measured over nearly the total flammability range for pentane, ethylene, and propyne in air.

3. Flame-front areas were measured, and the effects of fuel concentration in air and hydrocarbon type on the area were studied.

4. Fundamental flame velocities were presented for pentane, ethylene, and propyne mixtures for the concentration range from 60 to 130 percent of stoichiometric in air.

5. Equilibrium flame temperature and equilibrium free radical-product concentrations were calculated for the total flammability range in air of pentane, ethylene, and propyne at atmospheric pressure.

## CONCLUSIONS

The following conclusions were made as a result of this investigation:

1. An active particle diffusion mechanism of flame propagation is consistent with the observed changes in flame velocity with fuel concentration in air for the three hydrocarbons studied, pentane, ethylene, and propyne.

2. A form of the Tanford and Pease equation, which includes a small constant flame velocity independent of diffusion, will predict the observed changes in flame velocity with hydrocarbon concentration in air over the range 70 to 130 percent of stoichiometric.

Lewis Flight Propulsion Laboratory
National Advisory Committee for Aeronautics
Cleveland, Ohio

## APPENDIX A

## ELECTRONIC TIMING EQUIPMENT

The function of the electronic timing apparatus is to measure the time interval required for a flame front to propagate between two points located a known distance apart in a glass combustion tube. A block diagram, figure 1(a), illustrates the processes involved. In practice the signal generator, timer gate, and counter are integral parts of a Potter model 451-B interval timer which is actuated by start and stop electrical pulses that must have a positive rise time of 50 volts per microsecond.



A pulse shaping circuit forms these pulses. Figure 1(c) is the schematic diagram of the pulse shaper which consists of two symmetrical signal channels that trigger an Eccles-Jordon flip-flop multivibrator, tube T4. Tubes T2A and T2B are base clippers and amplifiers. A variable cathode bias, common to both tubes, determines the clipping level such that the lower level signals consisting of hum, noise, etc. can be blocked whereas the useful signal is amplified. Diodes T3A and T3B couple the clipper-amplifier tubes to the multivibrator tubes in such a manner that only the negative part of a signal appears at the multivibrator grids. At a given time one triode only may conduct in the Eccles-Jordon multivibrator circuit but two conditions of stability exist with one or the other triode active. After it has been set properly with the right triode in figure 1(c) conducting by a momentary closing of the reset switch, a negative signal from the "start" channel of the pulse shaper will trigger the multivibrator into the other stable condition and a negative signal from the "stop" channel will trigger it back to the original stable condition. Although the resistance capacitance input circuit of the Potter timer may alter the step waves of voltage thus generated in the plate circuits of the multivibrator, the requisite 50 volt per microsecond rise time of the wave front for which the multivibrators were designed will not be changed. Triodes T1A and T1B are cathode followers which isolate the clipper-amplifier tubes from the preceding high impedance amplifiers of the flame detectors.

The circuit diagram is shown in figure 1(b) for one of the two similar flame detectors which drive the dual channel shaper with "start" and "stop" signals. The phototube and its amplifiers are housed together in a metal box with careful shielding of components to minimize pick-up voltages and provide a relatively large signal to transmit to the pulse shaper. The outputs of the flame detectors are connected to the pulse shaper inputs with shielded cables which also carry power to the detectors from the power supply on the pulse shaper chassis. A slotted bakelite block mounted on one side of the detector box provides an aperture for limiting the portion of the combustion tube viewed by the

phototube to a very narrow section immediately in front. Use of direct coupling between the phototube and first amplifier and a very high phototube load-impedance results in maximum sensitivity. Low plate voltage on the first amplifier minimizes grid current. To reduce hum direct-current filament voltage is used on the amplifier tubes in the flame detector unit.

Bias for the multivibrator T4 in the pulse shaper is correct when one plate is negative about 25 volts with respect to ground and the other is near ground potential. The bias control (clipping level adjustment) for T2A and T2B then can be adjusted to eliminate noise or hum at the plates of T2A and T2B. Incorrect adjustment is apparent either as over-all low sensitivity or erratic timer operation with no light signals. This control adjustment is not critical. An approximate evaluation of the sensitivity can be formed from the fact that a 1/4-inch-diameter alcohol flame moved past the phototube at 3-inch distance is the minimum light input for operation of the system. Because of the direct coupling between the phototube and first amplifier, the system must be used in a dark room.

## APPENDIX B

## SYMBOLS

The following symbols are used in this report:

| | |
|---|---|
| $A_f$ | flame front area, sq cm |
| $A_t$ | cross-sectional area of flame tube, sq cm |
| $B_H$ | recombination factor for hydrogen atoms |
| $B_i$ | term arising from recombination of the $i^{th}$ active particles |
| D | diffusion coefficient |
| $D_i$ | rate of diffusion of the $i^{th}$ active particle, sq cm/sec |
| $D_H$ | diffusion coefficients for hydrogen atoms into air at room temperature, sq cm/sec |
| $D_O$ | diffusion coefficient for oxygen atoms into air at room temperature, sq cm/sec |
| $D_{OH}$ | diffusion coefficient for hydroxyl radicals into air at room temperature, sq cm/sec |
| h | one half the Boltzmann's constant times temperature |
| k | average specific rate constant for reaction of active particles and hydrocarbon molecules, cc molecules$^{-1}$ sec$^{-1}$ |
| $k_i$ | specific rate constant for reaction of combustible and the $i^{th}$ active particle, cc molecules$^{-1}$ sec$^{-1}$ |
| L | number of molecules of gas at reaction temperature, molecules/cc |
| $m_1, m_2$ | molecular masses |
| $N_1, N_2$ | molecular densities |
| n | number of molecules of final combustion products (combined $CO_2$ and $H_2O$) per molecule of fuel |
| $P_H$ | partial pressure of hydrogen atoms, atm |
| $P_i$ | partial pressure of the $i^{th}$ active particle, atm |

$P_O$ partial pressure of oxygen atoms, atm

$P_{OH}$ partial pressure of hydroxyl radicals, atm

$Q$ mole fraction of potential combustion product

$Q'$ mole fraction of combustible

$q_{O_2}$ 0.5 of the factor initial mole fraction of oxygen minus final mole fraction of oxygen

$U_f$ fundamental flame velocity, defined as velocity component normal to any tangent to flame surface, cm/sec

$U_g$ gas velocity, cm/sec

$U_O$ intercept of curve; 5.8 cm/sec for pentane, 15.1 cm/sec for ethylene, and 16.5 cm/sec for propyne

$U_o$ spatial flame velocity, cm/sec

$\theta_m$ 0.7 of equilibrium temperature over initial temperature

$\sigma$ arithmetic average of molecular diameters of diffusing gases



## REFERENCES

1. Simon, Dorothy Martin: Flame Propagation. III. Theoretical Consideration of the Burning Velocities of Hydrocarbons. Jour. Am. Chem. Soc., vol. 73, no. 1, Jan. 1951, pp. 422-425.

2. Simon, Dorothy Martin: On the Active Particle Diffusion Theory of Flame Propagation. Presented before a Joint Symposium on Combustion Chemistry of the Division of Petroleum Chemistry. Am. Chem. Soc. (Cleveland), April 9-12, 1951.

3. Tanford, Charles, and Pease, Robert N.: Theory of Burning Velocity. II. The Square Root Law for Burning Velocity. Jour. Chem. Phys., vol. 15, no. 12, Dec. 1947, pp. 861-865.

4. Semenov, N. N.: Thermal Theory of Combustion and Explosion. III. Theory of Normal Flame Propagation. NACA TM 1026, 1942.

5. Zeldovich, Y., and Semenov, N.: Kinetics of Chemical Reactions in Flames. NACA TM 1084, 1946.

6. Zeldovich, Y. B.: Theory of Combustion and Detonation of Gases. Tech. Rep. F-TS-1226-IA (GDAM A9-T-45), Air Materiel Command, 1949. (Trans. by Brown Univ.)

7. Hirschfelder, J. O., and Curtiss, C. F.: Theory of Propagation of Flames. Part I: General Equations, Third Symposium on Combustion and Flame and Explosion Phenomena, The Williams & Wilkins Co. (Baltimore), 1949, pp. 121-127.

8. Bechert, Karl: Zur Theorie der Verbrennungsgeschwindigkeit, mit einer Anwendung auf die Ozonverbrennung. Ann. der Physik, Folge 6, Bd. 4, Heft 5, 1949, S. 191-230.

9. Manson, N.: Mécanisme de la propagation des déflagrations dans les mélanges gazeux et role de la projection des centres actifs. Revue de L'Institut Francais du Petrole et Annales des Combustibles Liquides, T. 4, No. 7, Juillet 1949, P. 338-354.

10. Gerstein, Melvin, Levine, Oscar, and Wong, Edgar L.: Fundamental Flame Velocities of Pure Hydrocarbons. I - Alkanes, Alkenes, Benzene, and Cyclohexane. NACA RM E50G24, 1950.

11. Coward, H. F., and Jones, G. W.: Limits of Inflammability of Gases and Vapors. Bull. 279, Bur. Mines, 1939.

12. Coward, H. F., and Payman, W.: Problems in Flame Propagation. Chem. Rev., vol. 21, no. 3, Dec. 1937, pp. 359-366.

13. Coward, H. F., and Hartwell, F. J.: Studies in the Mechanism of Flame Movement. Part II - The Fundamental Speed of Flame in Mixtures of Methane and Air. Jour. Chem. Soc. (London), pt. II, 1932, pp. 2676-2684.

14. Burke, Edward, and Friedman, Raymond: Measurement of Burning Velocities of Acetylene and Dideuteroacetylene in Air. Presented before a Joint Symposium on Combustion Chemistry of the Division of Petroleum Chemistry. Am. Chem. Soc. (Cleveland), April 9-12, 1951.

15. Linnett, J. W., and Hoare, M. F.: Burning Velocities in Ethylene-Air Nitrogen Mixtures. Third Symposium on Combustion and Flame and Explosion Phenomena, The Williams & Wilkins Co. (Baltimore), 1949, pp. 195-204.

16. Linnett, J. W., and Hoare, M. F.: Burning Velocity Determination. Part III. - Burning Velocities of Ethylene + Air + Carbon Dioxide Mixtures. Trans. Faraday Soc. (London), vol. 47, pt. 2, Feb. 1951, pp. 179-183.

2267

17. Levine, Oscar, Wong, Edgar L., and Gerstein, Melvin: Fundamental Flame Velocities of Pure Hydrocarbons. II - Alkadienes. NACA RM E50H25, 1950.

18. Gerstein, Melvin, Levine, Oscar, and Wong, Edgar L.: Fundamental Flame Velocities of Hydrocarbons. Presented before a Joint Symposium on Combustion Chemistry of the Division of Petroleum Chemistry. Am. Chem. Soc. (Cleveland), April 9-12, 1951.

19. Lewis, Bernard, and von Elbe, Guenther: On the Theory of Flame Propagation. Jour. Chem. Phys., vol. 2, no. 8, Aug. 1934, pp. 537-546.

20. Tanford, Charles: Theory of Burning Velocity. I. Temperature and Free Radical Concentrations Near the Flame Front, Relative Importance of Heat Conduction and Diffusion. Jour. Chem. Phys., vol. 15, no. 7, 1947, pp. 433-439.

21. Tanford, Charles: The Role of Free Atoms and Radicals in Burner Flames. Third Symposium on Combustion and Flame and Explosion Phenomena, The Williams & Wilkins Co. (Baltimore), 1949, pp. 140-146.

22. Huff, Vearl N., and Morrell, Virginia E.: General Method for Computation of Equilibrium Composition and Temperature of Chemical Reactions. NACA TN 2113, 1950.

23. Huff, Vearl N., and Gordon, Sanford: Tables of Thermodynamic Functions for Analysis of Aircraft-Propulsion Systems. NACA TN 2161, 1950.

24. Anon.: Selected Values of Properties of Hydrocarbons. Circular C461, Nat. Bur. Standards, Nov. 1947.

25. Hottel, H. C., Williams, G. E., and Satterfield, C. N.: Thermodynamic Charts for Combustion Processes. Part I. John Wiley & Sons, Inc., 1949.

26. Huff, Vearl N., and Calvert, Clyde S.: Charts for the Computation of Equilibrium Compositions of Chemical Reactions in the Carbon-Hydrogen-Oxygen-Nitrogen System at Temperatures from 2000° to 5000° K. NACA TN 1653, 1948.

27. Jones, G. W., Lewis, Bernard, Friauf, J. B., and Perrott, G. St. J.: Flame Temperatures of Hydrocarbon Gases. Jour. Am. Chem. Soc., vol. 53, no. 3, March 1931, pp. 869-883.

28. Jeans, Sir James: An Introduction to the Kinetic Theory of Gases. Cambridge Univ. Press (London), p. 207.

TABLE I - SOURCE AND PURITY OF HYDROCARBONS

| Hydrocarbon | Source | Purity (percent) |
|---|---|---|
| Ethylene | Ohio Chemical and Mfg. Co. | 99 |
| Propyne | National Bureau of Standards | 98 |
| Pentane | (1) | 99.3 |

[1]Prepared jointly by NACA and National Bureau of Standards.

TABLE II - FLAME VELOCITIES

| Hydrocarbon | Percent stoichiometric | Spatial flame velocity $U_o$ (cm/sec) | Spatial flame velocity minus gas velocity $U_o-U_g$ (cm/sec) | Flame front area $A_f$ (sq cm) | Relative fundamental flame velocity $U_f$ (cm/sec) | Adjusted fundamental flame velocity $U'_f$ (cm/sec) |
|---|---|---|---|---|---|---|
| Ethylene | 59 | 44.5 | 44.5 | 10.20 | 21.4 | 23.0 |
| | 65 | 66.7 | 61.5 | 10.55 | 28.6 | 30.8 |
| | 76 | 103.5 | 89.6 | 10.90 | 40.4 | 43.5 |
| | 85 | 131.9 | 111.3 | 11.24 | 49.1 | 52.8 |
| | 93 | 153.3 | 127.6 | 11.49 | 54.6 | 58.8 |
| | 94 | 153.8 | 128.0 | 11.50 | 54.6 | 58.8 |
| | 101 | 174.6 | 143.9 | 11.68 | 60.5 | 65.1 |
| | 109 | 183.3 | 150.6 | 11.80 | 62.7 | 67.5 |
| | 117 | 185.1 | 151.9 | 11.84 | 63.0 | 67.8 |
| | 126 | 175.4 | 144.5 | 11.60 | 61.2 | 65.9 |
| | 137 | 160.6 | 133.2 | 11.27 | 58.1 | 62.5 |
| | 146 | 127.6 | ----- | ----- | ---- | ---- |
| | 157 | 87.6 | ----- | ----- | ---- | ---- |
| | 168 | 59.5 | ----- | ----- | ---- | ---- |
| | 178 | 47.4 | ----- | ----- | ---- | ---- |
| | 189 | 36.4 | ----- | ----- | ---- | ---- |
| | 202 | 33.8 | ----- | ----- | ---- | ---- |
| | 224 | 26.9 | ----- | ----- | ---- | ---- |
| | 234 | 25.4 | ----- | ----- | ---- | ---- |
| Pentane | 67 | 32.1 | 32.1 | 10.55 | 14.9 | 16.0 |
| | 82 | 61.5 | 56.5 | 11.14 | 24.9 | 26.8 |
| | 96 | 85.0 | 75.4 | 11.55 | 32.0 | 34.4 |
| | 110 | 94.8 | 82.9 | 11.80 | 34.5 | 37.1 |
| | 122 | 89.8 | 79.1 | 11.79 | 32.9 | 35.4 |
| | 137 | 66.6 | 61.4 | 11.36 | 26.5 | 28.5 |
| | 159 | 47.4 | ---- | ----- | ---- | ---- |
| | 178 | 32.8 | ---- | ----- | ---- | ---- |
| | 204 | 24.5 | ---- | ----- | ---- | ---- |
| Propyne | 59 | 45.0 | 44.9 | 10.20 | 21.6 | 23.2 |
| | 69 | 79.7 | 71.4 | 10.64 | 32.9 | 35.4 |
| | 80 | 117.1 | 100.0 | 11.06 | 44.4 | 47.8 |
| | 89 | 146.5 | 122.4 | 11.37 | 52.9 | 56.9 |
| | 100 | 164.6 | 136.2 | 11.65 | 57.4 | 61.8 |
| | 110 | 182.0 | 149.5 | 11.80 | 62.2 | 66.9 |
| | 119 | 182.9 | 150.3 | 11.79 | 62.6 | 67.4 |
| | 132 | 165.0 | 136.5 | 11.45 | 58.5 | 63.0 |
| | 145 | 141.9 | ----- | ----- | ---- | ---- |
| | 151 | 119.7 | ----- | ----- | ---- | ---- |
| | 164 | 82.1 | ----- | ----- | ---- | ---- |
| | 177 | 53.3 | ----- | ----- | ---- | ---- |
| | 188 | 38.3 | ----- | ----- | ---- | ---- |
| | 201 | 35.8 | ----- | ----- | ---- | ---- |
| | 214 | 30.7 | ----- | ----- | ---- | ---- |
| | 247 | 22.6 | ----- | ----- | ---- | ---- |

TABLE III - FREE ATOM AND RADICAL CONCENTRATIONS, AND EQUILIBRIUM FLAME TEMPERATURES

| Hydrocarbon | Hydrocarbon by volume in air (percent) | Hydrocarbon in air, percent stoichiometric | Equilibrium flame temperature $^{o}K$ (atm) | Equilibrium hydrogen atom concentration $P_H$ (atm) | Equilibrium oxygen atom concentration $P_O$ (atm) | Equilibrium hydroxyl radical concentration $P_{OH}$ (atm) |
|---|---|---|---|---|---|---|
| Pentane | 1.40 | 54 | 1591 | $0.0000\times10^{-3}$ | $0.004\times10^{-3}$ | $0.098\times10^{-3}$ |
| | 1.50 | 58 | 1670 | .0003 | .0122 | .199 |
| | 2.00 | 77 | 2013 | .0236 | .166 | 1.324 |
| | 2.60 | 101 | 2278 | .523 | .333 | 2.73 |
| | 2.67 | 107 | 2284 | .631 | .264 | 2.46 |
| | 2.78 | 108 | 2277 | .760 | .1583 | 1.91 |
| | 3.00 | 117 | 2226 | .819 | .0431 | .955 |
| | 3.17 | 124 | 2173 | .746 | .0144 | .52 |
| | 3.26 | 128 | 2148 | .699 | .0088 | .40 |
| | 3.43 | 135 | 2091 | .577 | .0029 | .21 |
| Ethylene | 3 | 44 | 1472 | $<0.0010\times10^{-3}$ | $0.0011\times10^{-3}$ | $0.0323\times10^{-3}$ |
| | 4 | 59 | 1796 | .0013 | .0369 | .3931 |
| | 5 | 75 | 2086 | .045 | .2995 | 1.793 |
| | 6 | 91 | 2303 | .411 | .759 | 3.805 |
| | 7 | 107 | 2391 | 1.271 | .561 | 3.704 |
| | 8 | 124 | 2347 | 1.708 | .128 | 1.732 |
| | 9 | 140 | 2246 | 1.444 | .0189 | .5957 |
| | 10 | 158 | 2140 | 1.007 | .0027 | .1047 |
| | 12 | 194 | 1932 | .349 | <.0010 | .0177 |
| | 15 | 251 | 1638 | .0362 | <.0010 | .0002 |
| Propyne | 2 | 39 | 1400 | $0.0000\times10^{-3}$ | $0.0004\times10^{-3}$ | $0.0139\times10^{-3}$ |
| | 3 | 59 | 1860 | .0026 | .0668 | .501 |
| | 4 | 79 | 2235 | .1618 | .715 | 2.85 |
| | 5 | 100 | 2439 | 1.151 | 1.267 | 4.90 |
| | 6 | 121 | 2468 | 2.398 | .555 | 3.455 |
| | 7 | 143 | 2388 | 2.578 | .0977 | 1.347 |
| | 8 | 165 | 2255 | 1.823 | .0096 | .3499 |
| | 9 | 188 | 2131 | 1.123 | .001 | .0872 |
| | 10 | 211 | 2053 | .790 | .0002 | .0299 |

TABLE IV - FLAME VELOCITIES PREDICTED BY EQUATION (6)

| Hydrocarbon | Hydrocarbon concentration in air, percent stoichiometric | Flame velocity | |
|---|---|---|---|
| | | Calculated (cm/sec) | Experimental (cm/sec) |
| Pentane $k_{av}=1.54\times10^{-13}$ | 67 | 16.6 | 16.0 |
| | 82 | 25.6 | 26.8 |
| | 96 | 33.0 | 34.4 |
| | 110 | 36.6 | 37.1 |
| | 122 | 35.2 | 35.4 |
| Ethylene $k_{av}=2.47\times10^{-13}$ | 59 | 26.3 | 23.0 |
| | 67 | 31.2 | 30.8 |
| | 76 | 40.7 | 43.5 |
| | 85 | 48.9 | 52.8 |
| | 94 | 57.1 | 58.8 |
| | 101 | 62.0 | 65.1 |
| | 109 | 67.1 | 67.5 |
| | 117 | 69.0 | 67.8 |
| | 126 | 68.5 | 65.9 |
| Propyne $k_{av}=1.7\times10^{-13}$ | 59 | 26.7 | 23.2 |
| | 69 | 34.8 | 35.4 |
| | 80 | 43.9 | 47.8 |
| | 89 | 52.2 | 56.9 |
| | 100 | 59.0 | 61.8 |
| | 110 | 64.8 | 66.9 |
| | 117 | 67.5 | 67.3 |
| | 132 | 69.3 | 67.0 |

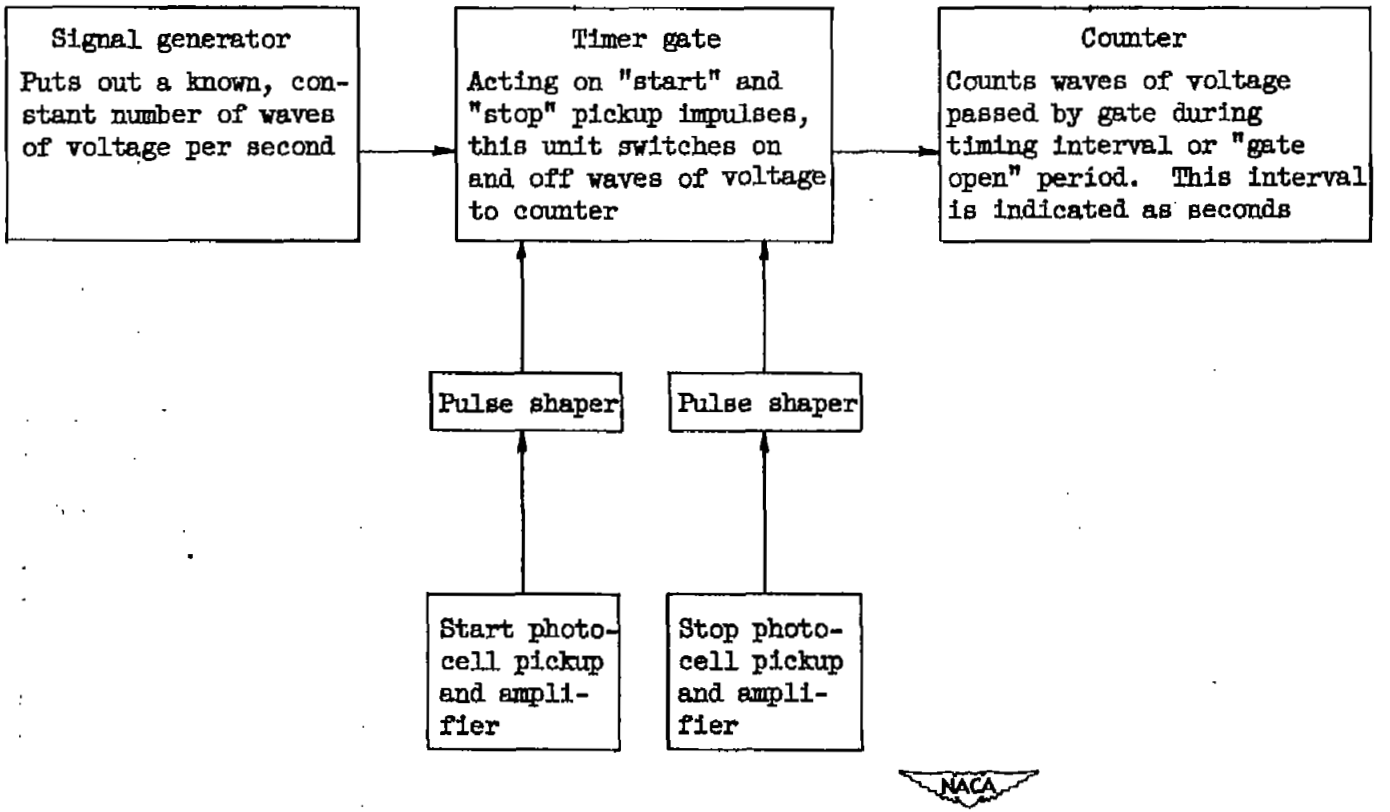


(a) Photoelectric timer.

Figure 1. - Schematic diagrams of circuits.

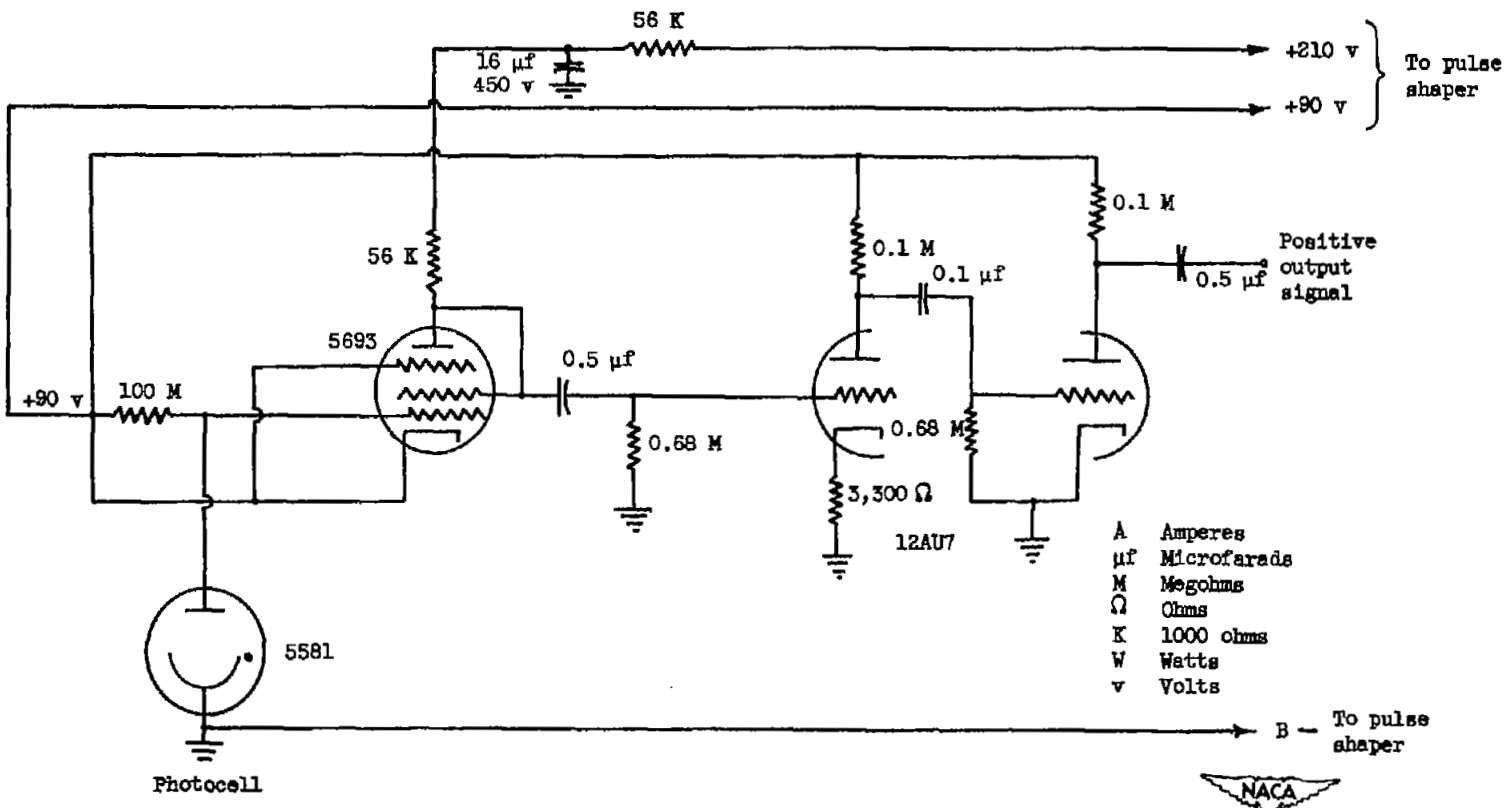


(b) Flame detector.

Figure 1. - Continued. Schematic diagrams of circuits.

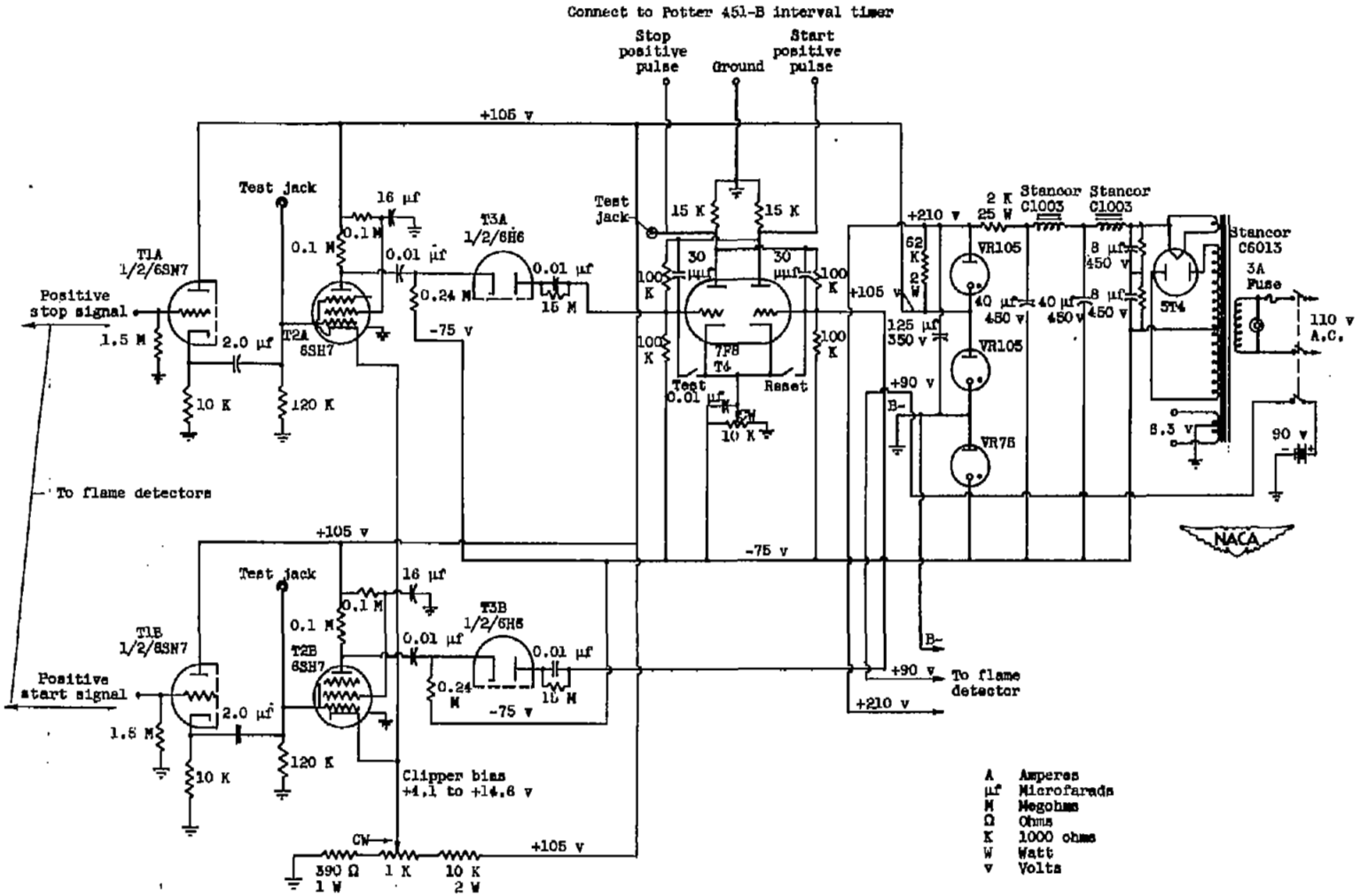


(c) Timer pulse shaper.

Figure 1. - Concluded. Schematic diagrams of circuits.

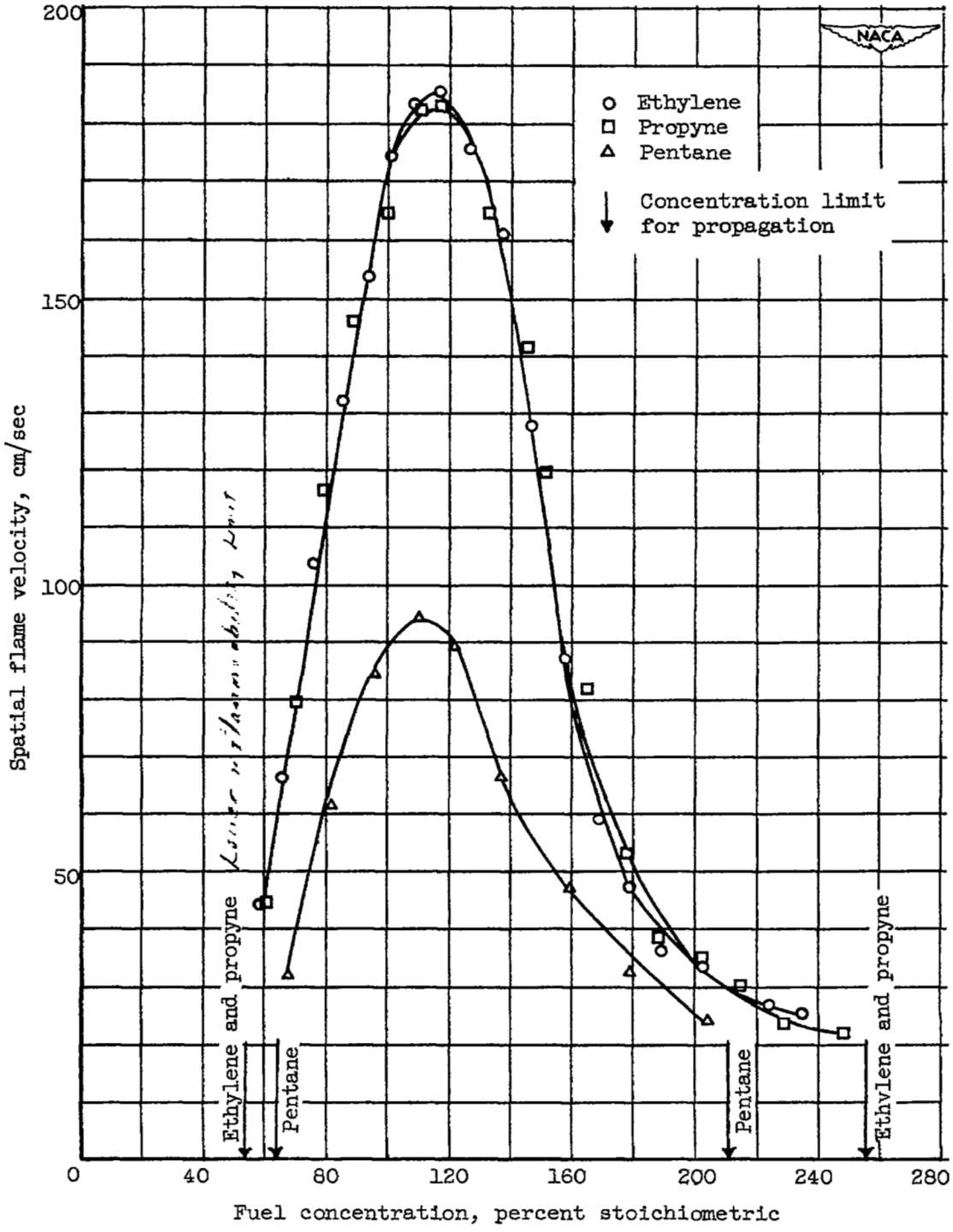


Figure 2. - Change in spatial flame velocity with mixture concentration.

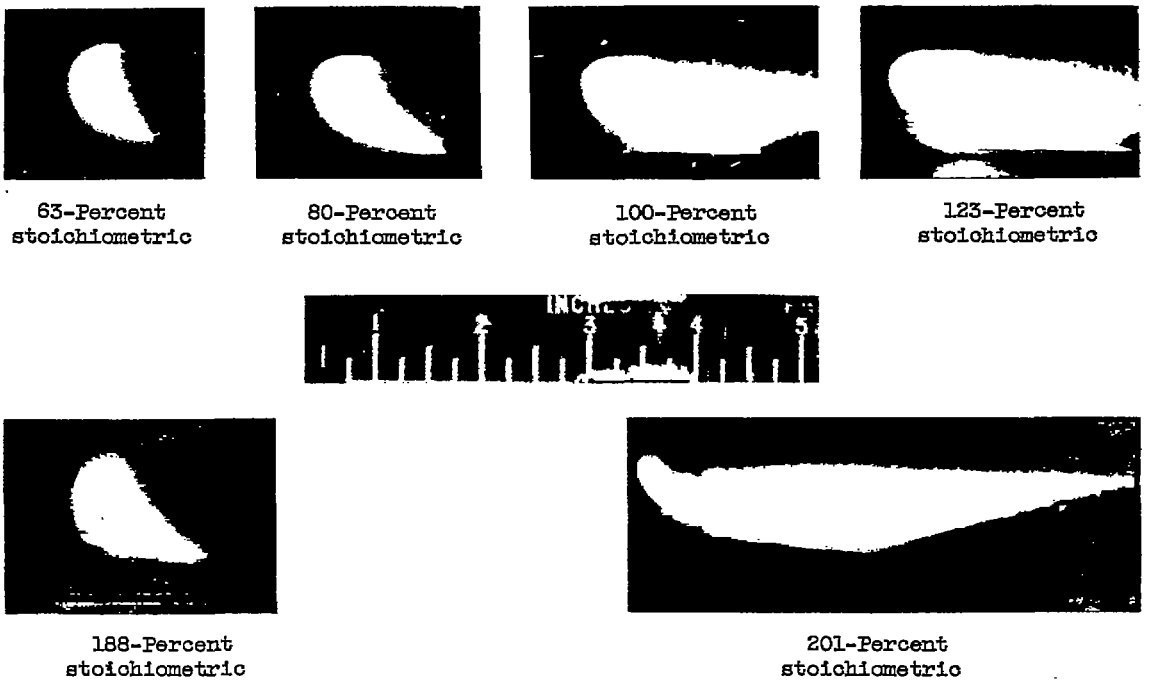


(a) Regular flame shapes for various fuel concentrations.

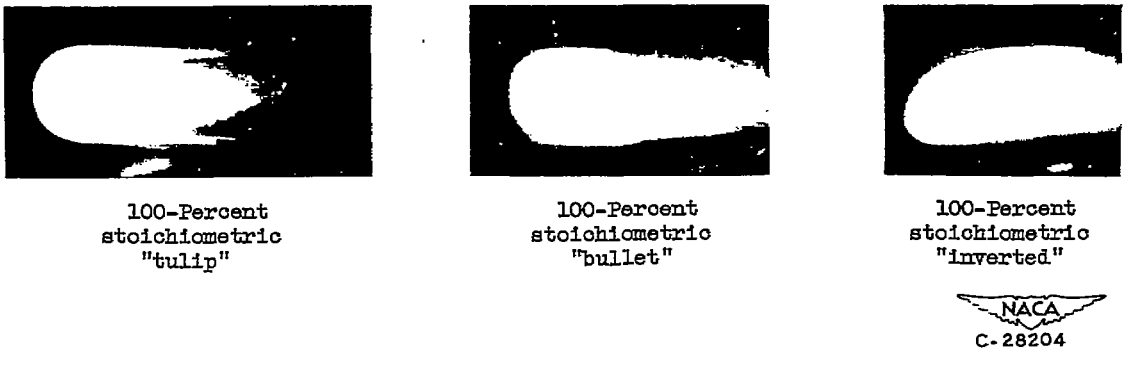


(b) Irregular flame shapes.

Figure 3. - Flame shapes for some propyne-air mixtures.

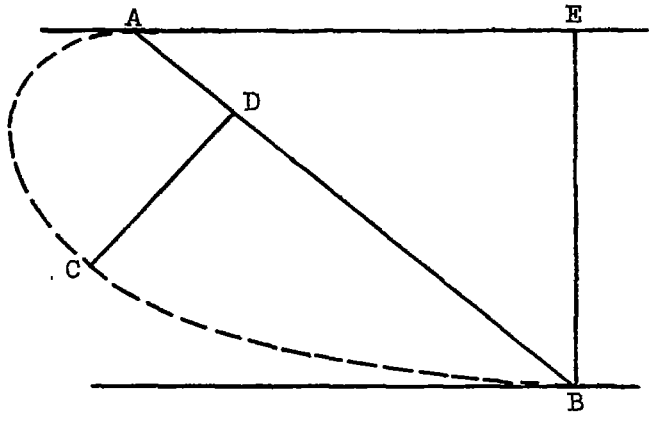


Figure 4. - Typical flame front trace.

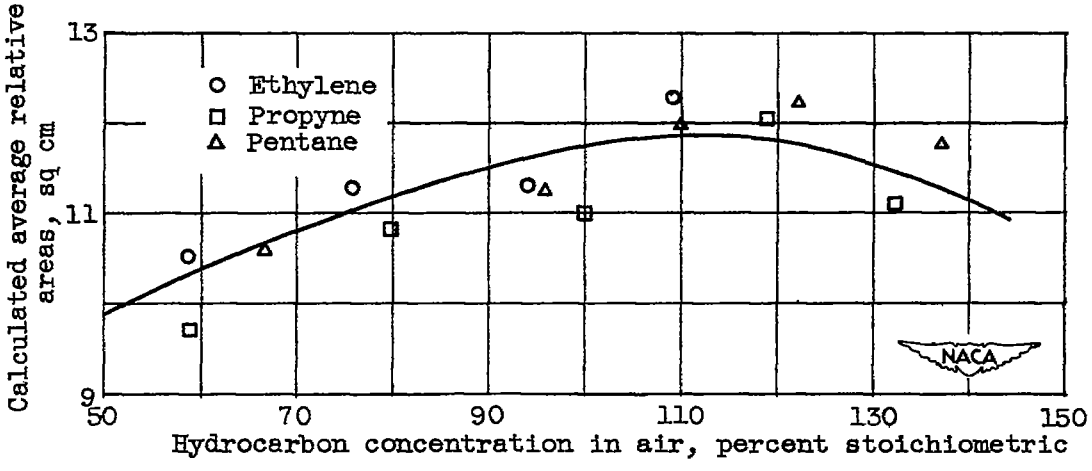


Figure 5. - Change in surface area with composition.

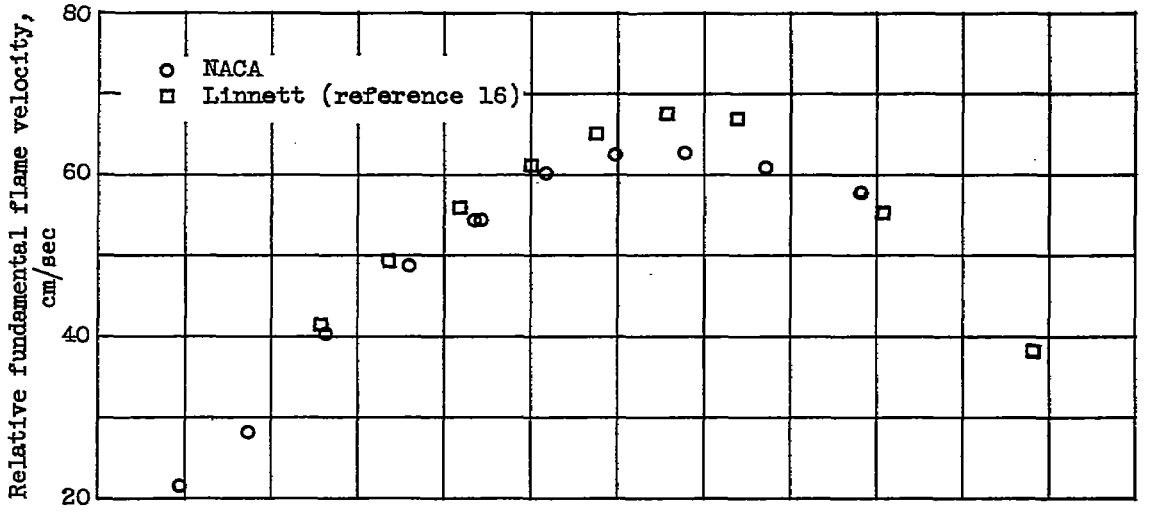


(a) Relative fundamental flame velocity.

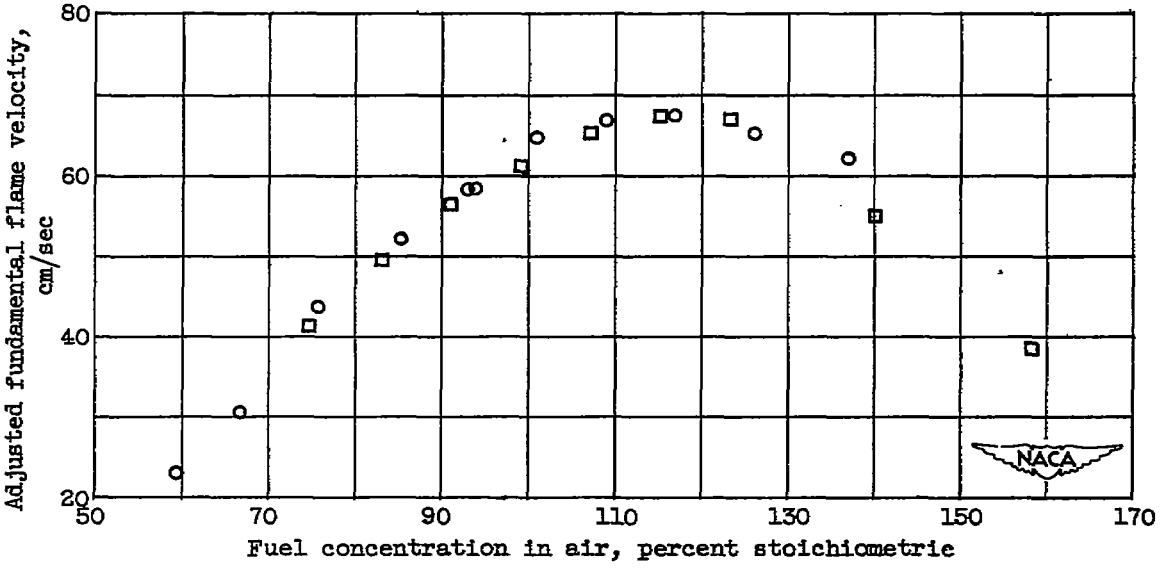


(b) Adjusted fundamental velocity.

Figure 6. - Comparison of fundamental flame velocity data for ethylene-air mixtures.

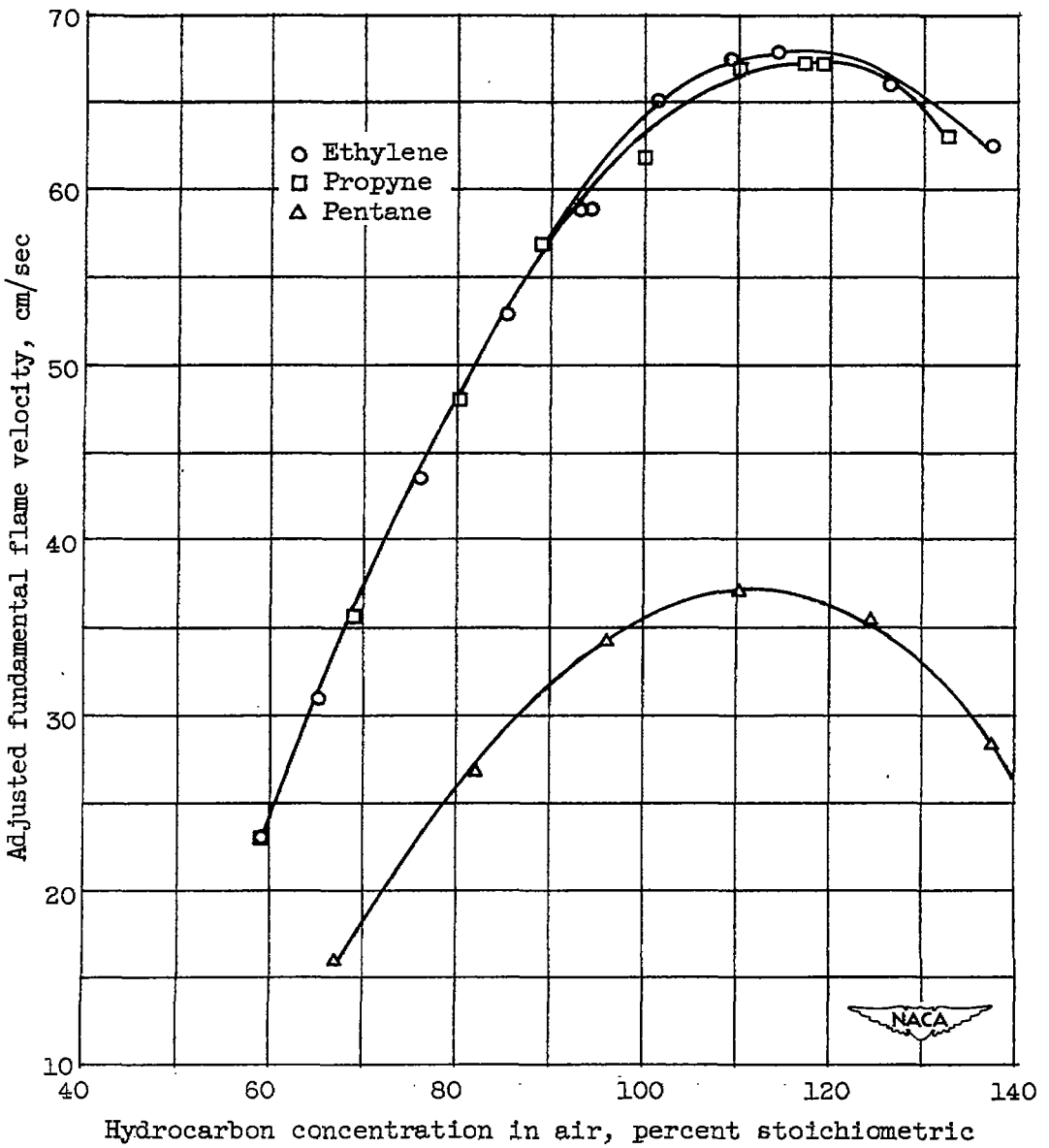


Figure 7. - Fundamental flame velocity.

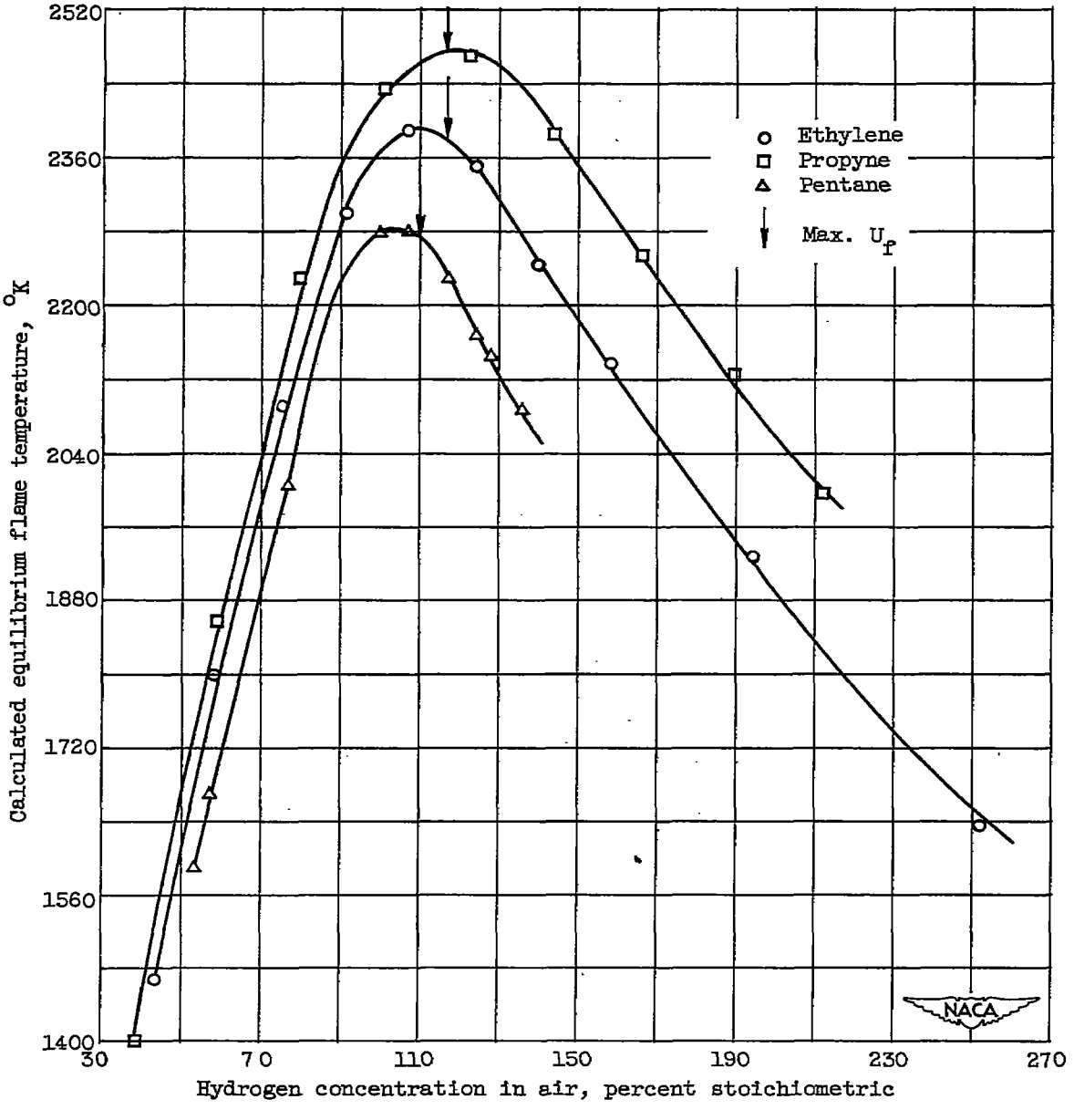


Figure 8. - Calculated equilibrium flame temperatures.

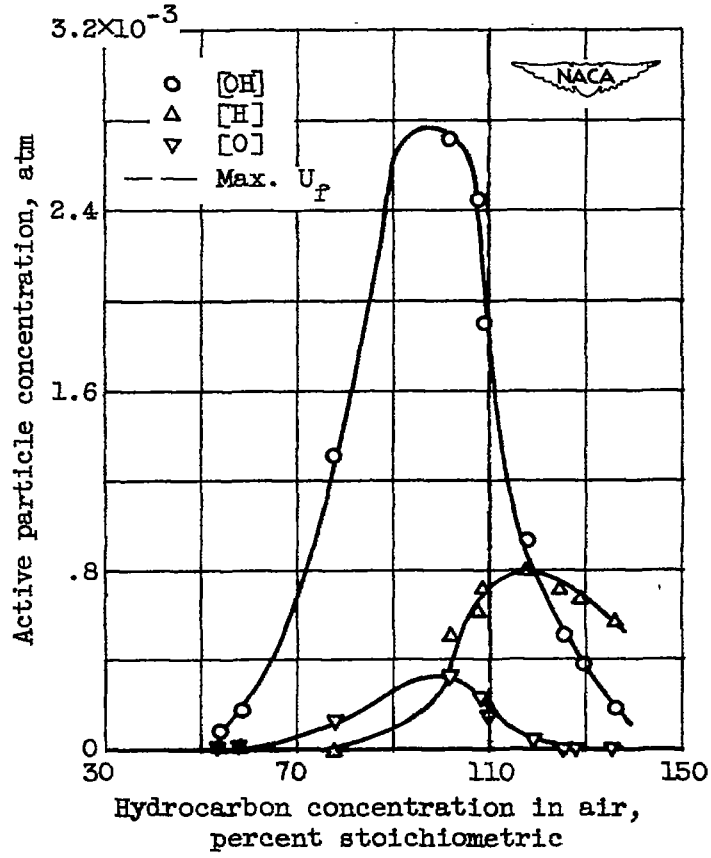


(a) Pentane.

Figure 9. - Calculated active particle concentrations.

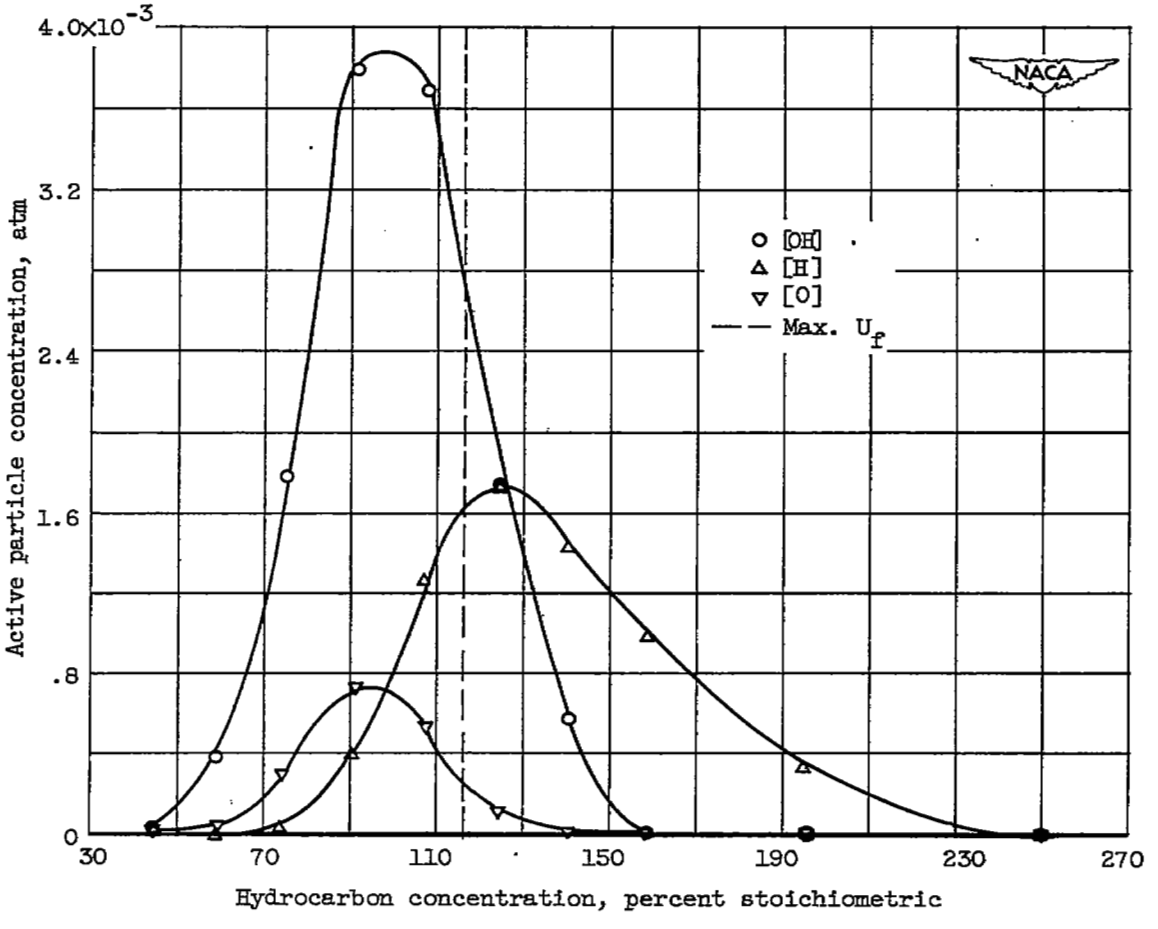


(b) Ethylene.

Figure 9. - Continued. Calculated active particle concentrations.

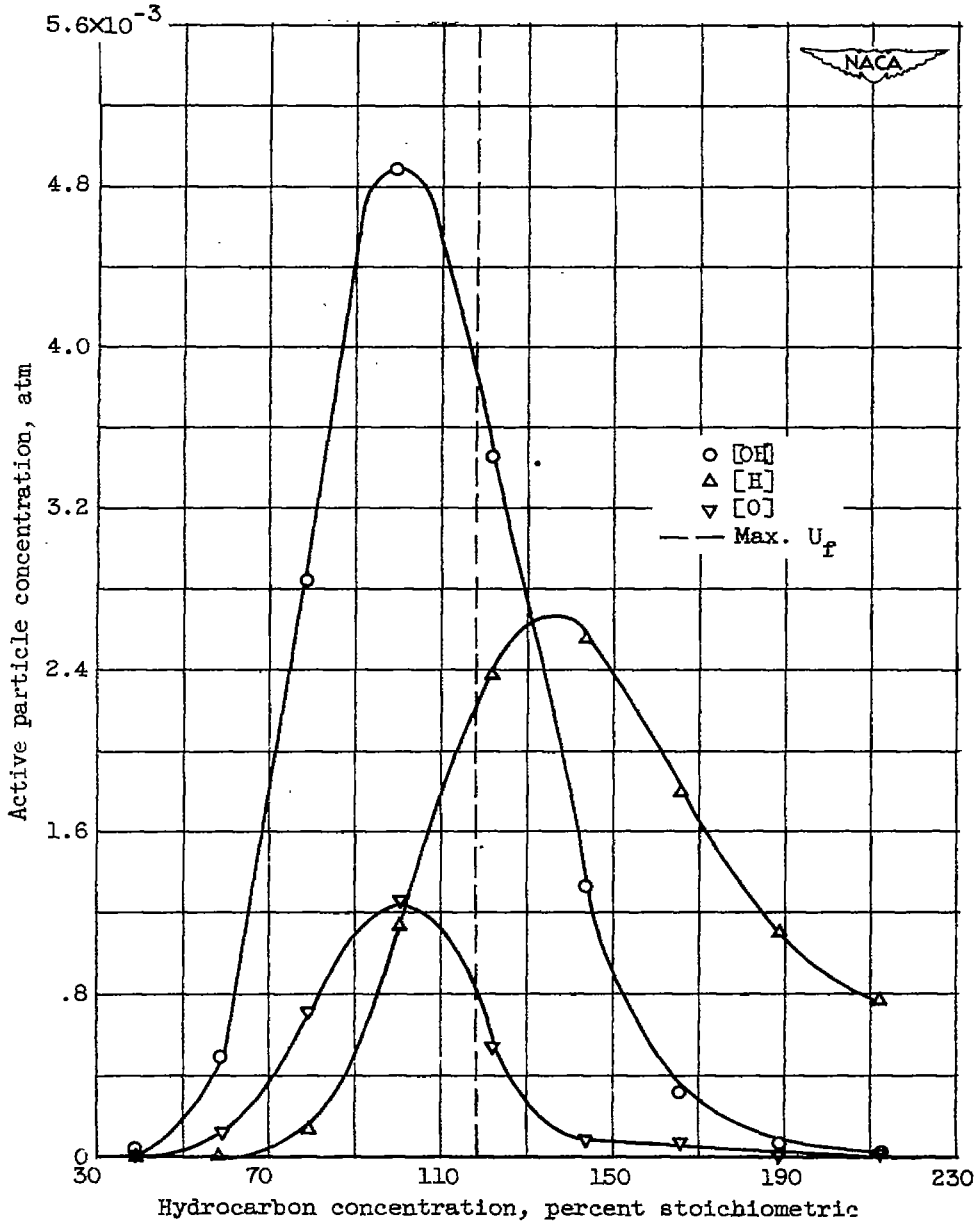


(c) Propyne.

Figure 9. - Continued. Calculated active particle concentrations.

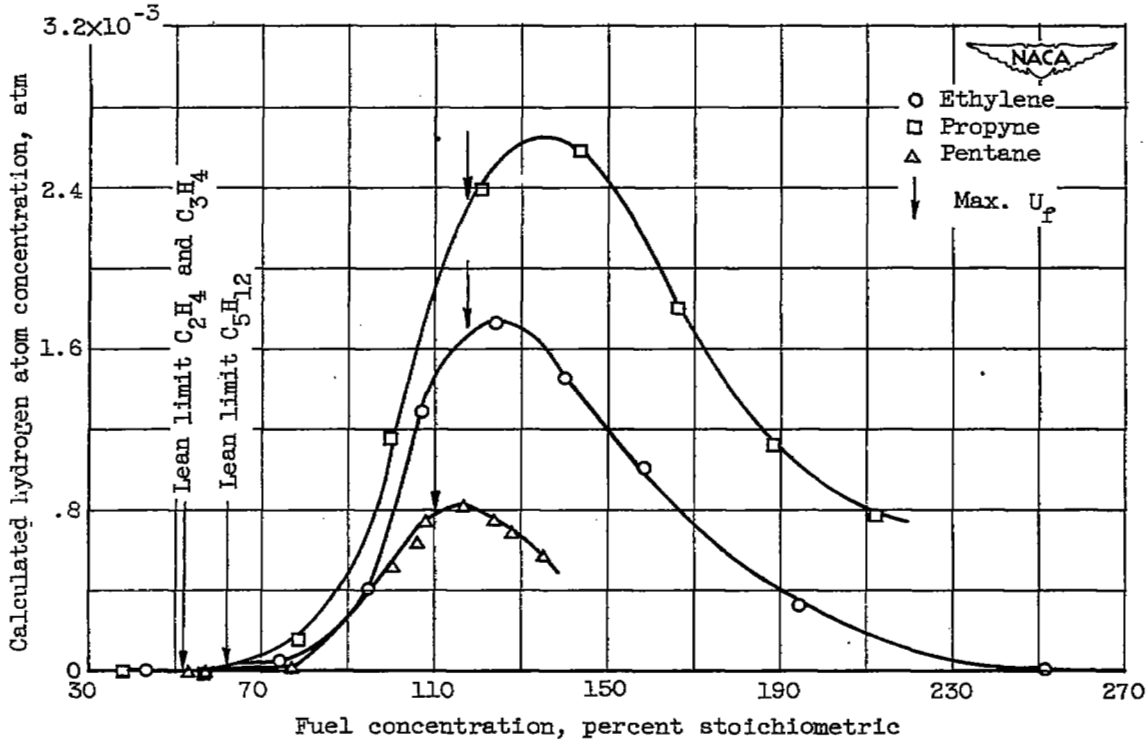


(d) Hydrogen atom concentrations for pentane, propyne, and ethylene.

Figure 9. - Concluded. Calculated active particle concentrations.

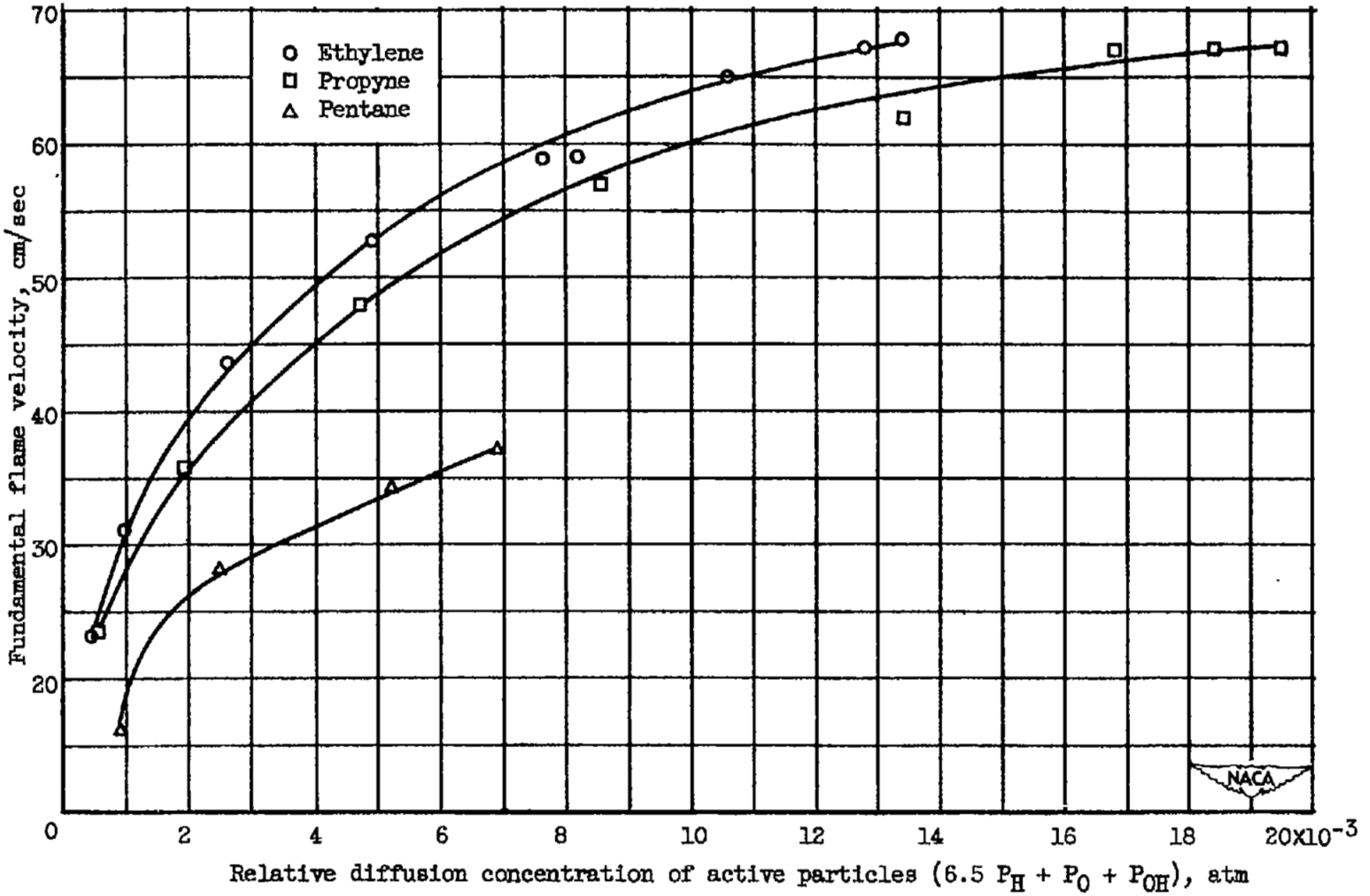


Figure 10. - Variation of fundamental flame velocity with relative diffusion concentration of active particles.

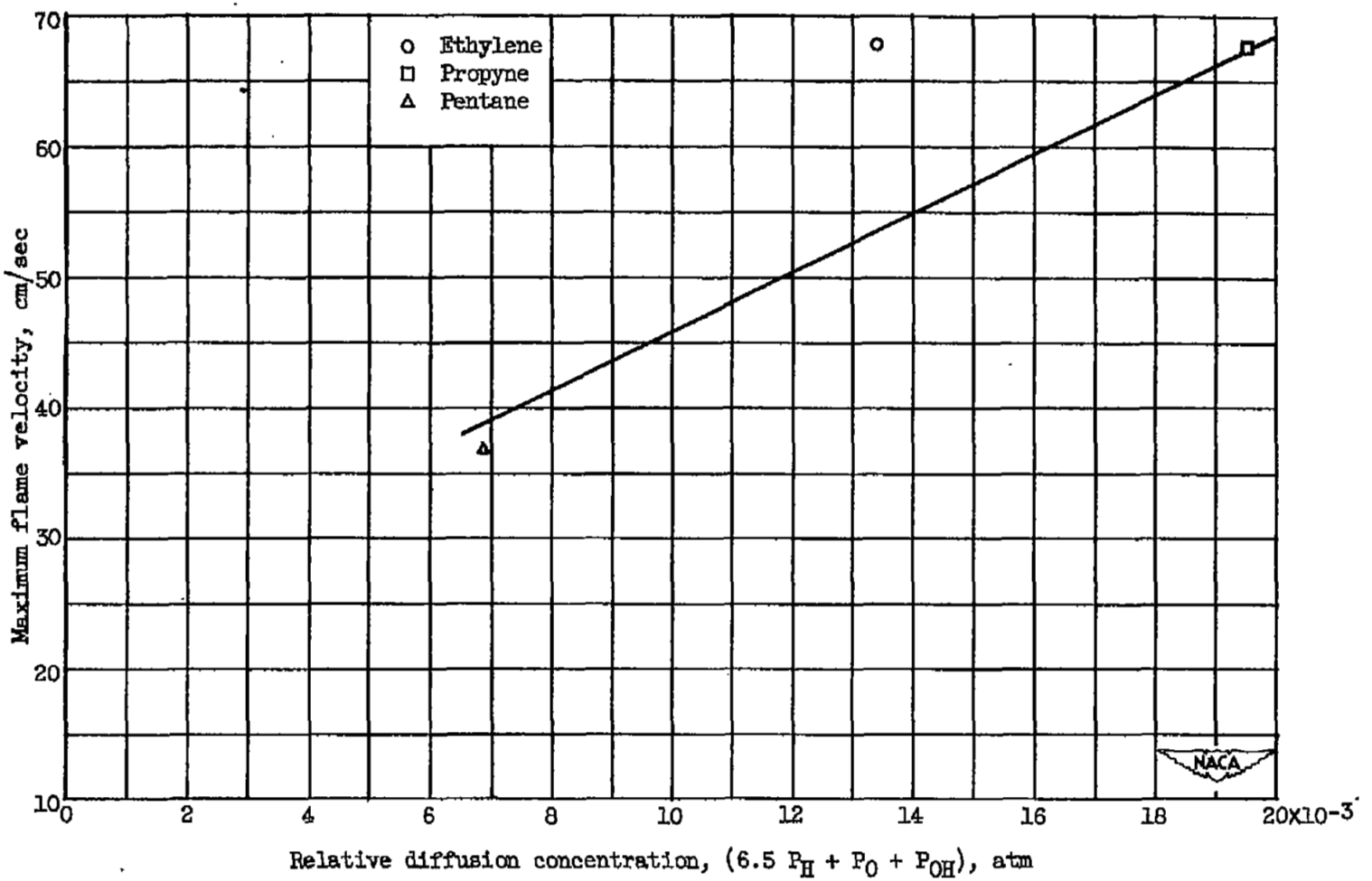


Figure 11. - Correlation for 52 hydrocarbons at maximum flame velocity (reference 2).

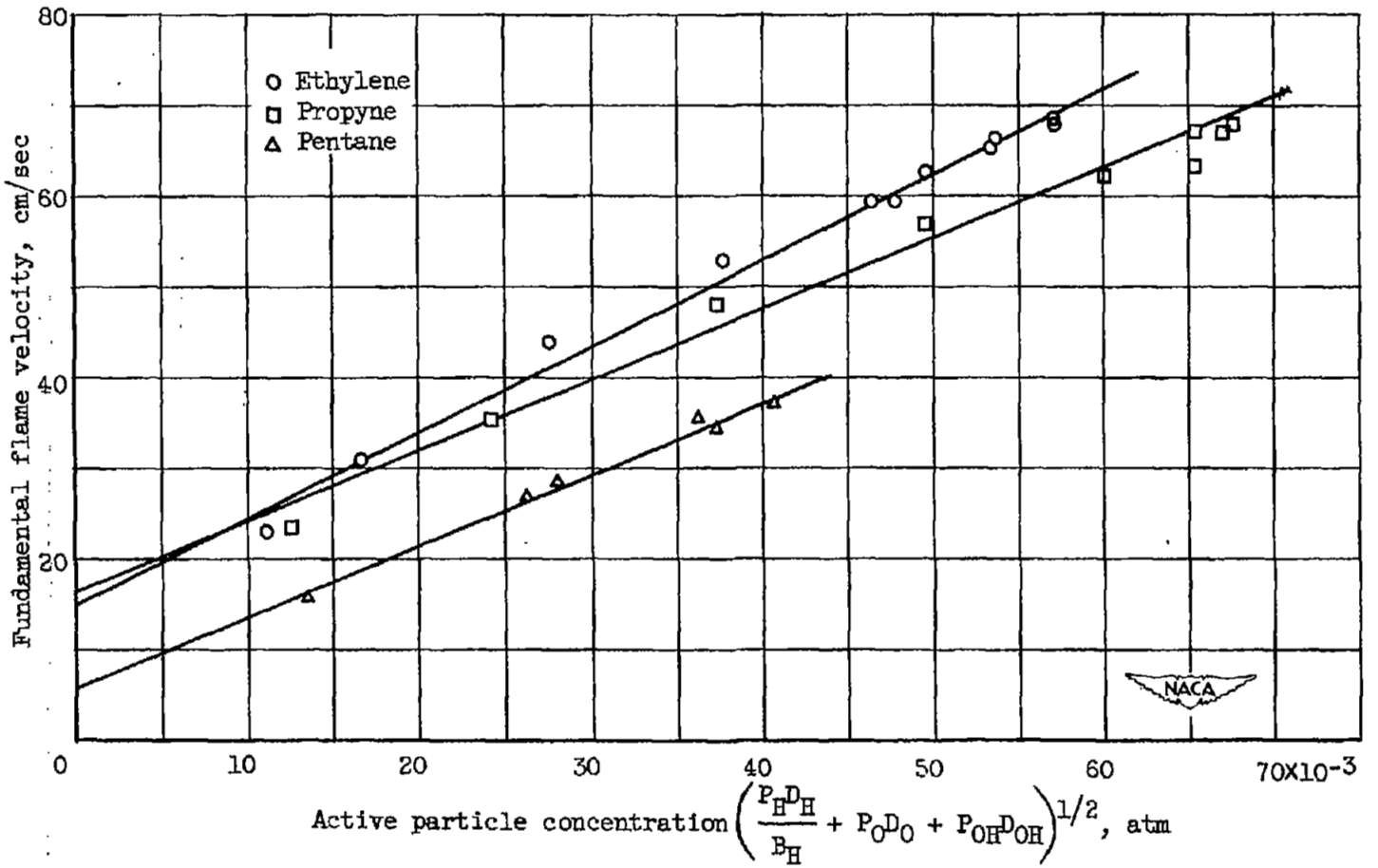


Figure 12. - Variation of flame velocity with square root of diffusion concentration of active particles.